



1 Biogeochemical Layering and Transformation of 2 Particulate Organic Carbon in the Tropical Northwestern 3 Pacific Ocean Inferred from $\delta^{13}\text{C}$

4 Authors

5 Detong Tian^{1,3}, Xuegang Li^{1,2,3,4*}, Jinming Song^{1,2,3,4*}, Jun Ma^{1,2}, Huamao Yuan^{1,2,3,4},
6 Liqin Duan^{1,2,3,4}

7 Affiliations

8 ¹CAS Key Laboratory of Marine Ecology and Environmental Sciences, Institute of Oceanology, Chinese
9 Academy of Sciences, Qingdao 266000, China

10 ²Laboratory for Marine Ecology and Environmental Science, Qingdao Marine Science and Technology
11 Center, Qingdao 266237, China

12 ³University of Chinese Academy of Sciences, Beijing 100049, China

13 ⁴Center for Ocean Mega-Science, Chinese Academy of Sciences, Qingdao 266000, China

14 *Corresponding to:* Xuegang Li (lixuegang@qdio.ac.cn) and Jinming Song (jmsong@qdio.ac.cn).

15 **Abstract.** Particulate organic carbon (POC) serves as the main carrier of the biological pump and
16 determines its transmission efficiency, yet the transformation processes of POC remain incompletely
17 understood. This study reports the vertical distribution of POC, dissolved inorganic carbon (DIC), $\delta^{13}\text{C}$ -
18 POC, and $\delta^{13}\text{C}$ -DIC in the tropical Northwestern Pacific Ocean (TNPO). The research identified three
19 distinct biogeochemical layers governing POC transformation: the POC rapid synthesis-degradation
20 layer (RSDL, 0-300 m), the net degradation layer (NDL, 300-1,000 m), and the stable layer (SL, 1,000-
21 2,000 m). From the top to the bottom of the RSDL, $\delta^{13}\text{C}$ -POC decreased by an average of 2.23‰, while
22 the carbon-to-nitrogen ratios (C:N) increased by an average of 2.3:1, indicating the selective degradation
23 of POC. In the NDL, $\delta^{13}\text{C}$ -POC and $\delta^{13}\text{C}$ -DIC exhibited a significant negative correlation ($r = 0.43$, $p <$
24 0.05), indicating a net transformation of POC to DIC. In the SL, POC proved to be resistant to
25 degradation, with POC exhibiting the highest C:N (15:1 on average) and the lowest $\delta^{13}\text{C}$ -POC (average
26 -27.71‰).

27 1 Introduction

28 As the most significant carbon reservoir on the earth's surface, the ocean absorbs about 2.6 billion tons
29 of carbon dioxide (CO_2) from the atmosphere each year, accounting for 25% of global anthropogenic
30 CO_2 emissions (Friedlingstein et al., 2023). After entering the ocean, CO_2 initially dissolves in seawater,
31 forming dissolved inorganic carbon (DIC). Subsequently, phytoplankton and photosynthetic bacteria at
32 the ocean surface convert it into organic carbon through photosynthesis. The majority of carbon in the
33 ocean is in the form of DIC, constituting over 98% of the total carbon content, with the remaining 2%



34 existing as POC and dissolved organic carbon (DOC). Despite being in minimal quantities, POC can be
35 transported to the deep ocean through the biological pump and buried for thousands of years. This process
36 of carbon sequestration aids in the absorption of CO₂ by the ocean, contributing to the regulation of
37 atmospheric CO₂ levels (Longhurst and Glen Harrison, 1989; Turner, 2015). Organic matter produced
38 from the euphotic layer is the primary food source for heterotrophic communities in the dark ocean (Smith
39 et al., 2008); once POC is exported from the euphotic layer, microorganisms rapidly utilize it, releasing
40 DIC (Song, 2010).

41 Some studies have shown that unstable components such as proteins and carbohydrates in POC are
42 preferentially degraded by microorganisms (Eadie and Jeffrey, 1973). However, conducting detailed
43 quantitative analyses of each POC component in actual investigations is challenging, necessitating the
44 use of alternative indicators to demonstrate selective degradation. The generally accepted indicator is the
45 carbon-to-nitrogen ratios (C:N) due to inherent differences in the C:N of various compounds in
46 POC (Morales et al., 2021). Thus, changes in the C:N during degradation can signify the selective
47 degradation of POC. Nevertheless, the composition of POC is highly complex, and the C:N of its
48 different components are not absolute. For example, lipids typically have a higher C:N than proteins, but
49 the opposite can also occur (Sannigrahi et al., 2005; Hernes and Benner, 2002). Therefore, relying solely
50 on the C:N to reflect the selective degradation process of POC has significant limitations. Although the
51 vital activities of the microbial community in the dark ocean are predominantly driven by heterotrophic
52 respiration (Herndl et al., 2023), many autotrophic organisms use chemical energy to synthesize POC.
53 Compelling evidence indicates that chemoautotrophy plays a substantial role in the fixation of DIC in
54 the minimum oxygen zone (OMZ) (Reinthal et al., 2010) and the deeper ocean (Passos et al., 2022;
55 Walsh et al., 2009). Consequently, there is a continuous conversion of POC and DIC throughout the
56 ocean water column. Exploring the degradation and synthesis of POC in the ocean is imperative to
57 enhance our comprehension of the biological pump processes.

58 The DIC in seawater primarily occurs in four chemical forms: H₂CO₃, HCO₃⁻, CO₃²⁻, and CO₂. In
59 comparison, the composition of POC is more complex. POC comprises various organic compounds
60 originating from living organisms such as phytoplankton, zooplankton, and microorganisms. It also
61 encompasses fecal particles, cell fragments, and diverse organic substances from external sources. Only
62 a small fraction of the POC has been accurately identified in terms of molecular structures (Kharbush et
63 al., 2020). As the depth increases, the readily degradable components in POC are used up, leading to a



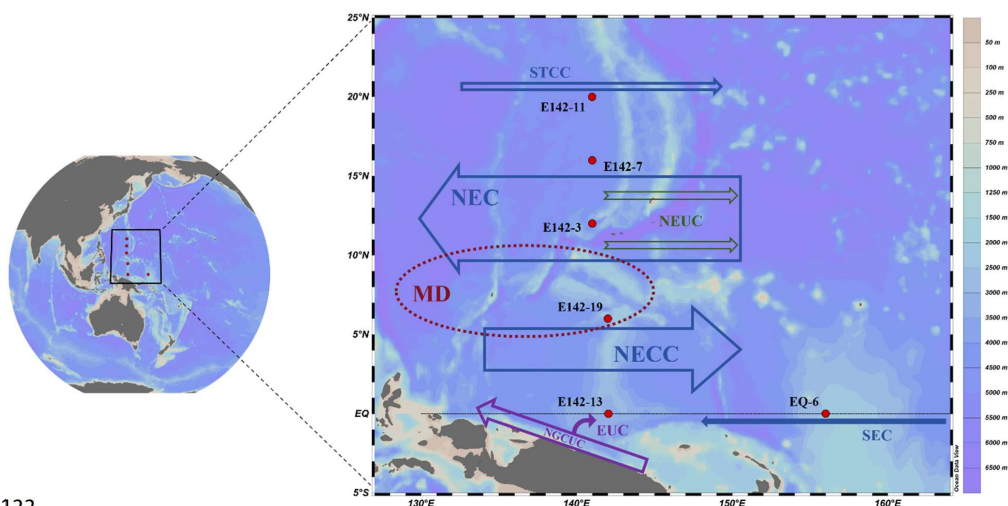
64 more intricate structure of the remaining POC through the transformation process. The remaining
65 refractory POC is even more difficult to identify(Lee et al., 2000). Therefore, it becomes challenging to
66 study the chemical characteristics of POC and its transformation process from itself. The $\delta^{13}\text{C}$ is a crucial
67 indicator that can reveal the origin, migration, and transformation of POC, making it significantly
68 important in the investigation of the marine carbon cycle(Ding et al., 2020; Jeffrey et al., 1983).
69 Compared with POC molecules, $\delta^{13}\text{C}$ -POC provides a more accurate reflection of the chemical properties
70 of the POC pool and the migration and transformation processes of POC(Close and Henderson, 2020).
71 Similarly, $\delta^{13}\text{C}$ -DIC can offer insights into important processes within the ocean carbon cycle. As POC
72 settles, it undergoes a series of biogeochemical processes, including synthesis, degradation, and
73 adsorption. Therefore, the isotope fractionation effect in POC is strong, resulting in significant
74 differences in $\delta^{13}\text{C}$ -POC values at different depths. In contrast, the fractionation of $\delta^{13}\text{C}$ -DIC is subject
75 to fewer influencing factors, and the DIC concentration in the ocean is notably high, thereby engendering
76 minimal variability in $\delta^{13}\text{C}$ -DIC across the ocean water column(Jeffrey et al., 1983). Therefore, $\delta^{13}\text{C}$ -
77 DIC is more sensitive to the fractionation effect in the ocean carbon cycle. Even slight variations in the
78 $\delta^{13}\text{C}$ -DIC value can reflect significant processes involved in the migration and transformation of
79 POC(Quay and Stutsman, 2003). Through the analysis of $\delta^{13}\text{C}$ -POC and $\delta^{13}\text{C}$ -DIC, we can enhance our
80 comprehension of the intricate composition, transport, and alteration mechanism of POC, providing us
81 with a more profound insight into the dynamic transformations within the ocean biological pump.

82 The tropical Northwestern Pacific Ocean (TNPO) is characterized by intricate current patterns and
83 water mass distributions(Hu et al., 2015; Schönau et al., 2022), and it is also known for the highest
84 surface seawater temperatures globally(Jia et al., 2018). High temperatures facilitate the respiration of
85 heterotrophic organisms, promoting the formation of biological hotspots and ultimately enhancing
86 material circulation and energy flow in the upper ocean(Guo et al., 2023; Iversen and Ploug, 2013). The
87 air-sea interaction within the TNPO is highly dynamic, exhibiting a shift from being a carbon sink to a
88 carbon source as it extends from higher to lower latitudes(Takahashi et al., 2009; Wu et al., 2005). The
89 complex hydrological characteristics, rapid elemental cycle, and frequent air-sea exchange render the
90 TNPO an ideal laboratory for exploring the ocean carbon cycle. In this research, we collected seawater
91 and particulate matter samples at six stations in the core and boundary regions of the TNPO, and the
92 relationship between DIC, POC, and their stable carbon isotopes was comprehensively analyzed to
93 enhance our understanding of the POC transformation process and the ocean carbon cycle process.



94 2 Sampling and Methods

95 The samples were collected in the TNPO during an expedition on R/V *Kexue* from March to April 2022.
96 A total of 6 stations were set up: EQ-6 (150.99° E, 0.00° N, 1944 m), E142-3 (140.99° E, 12.01° N, 4091
97 m), E142-7 (140.99° E, 15.99° N, 4725 m), E142-11 (140.99° E, 20.00° N, 462 4m), E142-13 (142.04°
98 E, 0.00° N, 3382 m) and E142-19 (141.99° E, 6.01° N, 2580 m) (Fig. 1). The 12-L Niskin bottles (KC-
99 Denmark, Denmark) mounted on a Conductivity-Temperature-Depth (CTD, Sea-bird SBE911, United
100 States) rosette was used to obtain water samples from the vertical profile of 0-2,000 m at each station for
101 analysis of temperature, salinity, dissolved oxygen (DO), POC, $\delta^{13}\text{C}$ -POC, particulate nitrogen (PN),
102 DIC, $\delta^{13}\text{C}$ -DIC, and chlorophyll a (Chl-*a*). The specific sampling and analysis methods are as follows.
103 **Temperature and salinity:** The temperature and salinity were measured by CTD (Sea-bird SBE911,
104 United States) in situ during sampling.
105 **DO:** Water samples were collected, fixed, and titrated according to the classic Winkler method, the
106 precision of which was 2.2×10^{-3} $\mu\text{mol/L}$ (Bryan et al., 1976; Zuo et al., 2018).
107 **POC, $\delta^{13}\text{C}$ -POC, and PN:** Particle samples were obtained by filtering 2-5 L of seawater onto a GF/F glass
108 filter (0.7 μm , Whatman) that had been combusted in a muffle furnace (450°C, 4 h) and acid-soaked
109 (0.5 M hydrochloric acid (HCl), 24 h). The filter was treated with HCl to remove inorganic carbonates
110 and oven-dried at 60°C. Afterward, POC, PN concentration, and $\delta^{13}\text{C}$ -POC were analyzed using an
111 elemental analyzer and an isotope mass spectrometer (Thermo Fisher Scientific Flash EA 1112 HT-Delta
112 V Advantages, United States) with an accuracy of $\pm 0.8\%$ and $\pm 0.2\%$, respectively (Ma et al., 2021).
113 **DIC:** Sampling was performed using a 50 ml glass bottle. After the water sample overflowed, 1 ml of
114 the sample was taken out with a pipette and then fixed with saturated mercuric chloride solution to
115 remove the influence of biological activity. The DIC concentration was measured using a DIC analyzer
116 (Apollo SciTech AS-C3, United States) with an accuracy of $\pm 0.1\%$ (Ma et al., 2020).
117 **$\delta^{13}\text{C}$ -DIC:** Automatic analysis was performed using a Thermo Delta-V isotope ratio mass spectrometer
118 (ThermoFisher Scientific MAT 253Plus, United States).
119 **Chl -*a*:** 2 L of water sample after zooplankton removal was filtered onto pre-combusted (450°C for 5 hr)
120 GF/F filters (0.7 μm , Whatman), extracted with 90% propanol for 12-24 h, and the concentration was
121 measured using a fluorescence photometer (Turner Designs, United States).



122

123 **Figure 1. TPWO sampling stations (red dots in the figure) and ocean current distribution. In the figure, blue**
124 **represents the ocean currents from the surface to the bottom of the thermocline, mainly STCC, NEC, NECC,**
125 **and SEC; green represents the ocean currents in the subthermocline, mainly NEUC; purple represents the**
126 **ocean currents from the bottom of the thermocline to the subthermocline, mainly EUC.**

127 3 Results and Discussion

128 3.1 Hydrological Characteristics

129 Except for station E142-11, the remaining five stations are all located at the Western Pacific Warm Pool
130 (WPWP). The SST of the five stations in the warm pool area was higher, averaging 29.01 ± 0.67 °C,
131 while station E142-11 had a lower SST of 25.02 °C. The strong seawater stratification in the study area
132 restricted the movement of nutrient-rich water from the deep to the upper ocean, resulting in the region
133 showing oligotrophic characteristics (Radenac et al., 2013). Therefore, the Chl-*a* concentration in the
134 DCM was notably low, with an average of only 0.24 ± 0.04 µg/L.

135 The study area is traversed by six major ocean currents: the South Equatorial Current (SEC), the North
136 Equatorial Current (NEC), the North Equatorial Undercurrent (NEUC), the Subtropical Countercurrent
137 (STCC), the Equatorial Undercurrent (EUC) and the North Equatorial Countercurrent (NECC). Among
138 them, the SEC flows from east to west along the equator and is characterized by high temperature and
139 low salinity, notably impacting station EQ-6. The NEC is a major westward current in the study area,
140 accompanied by a series of eastward undercurrents of NEUC in its lower part; stations E142-3 and E142-
141 7 are mainly affected by them. The STCC is characterized by a multi-eddy structure that flows eastward



142 in the subtropical region of the North Pacific and notably impacts station E142-11. The EUC is a strong
143 eastward current rich in oxygen and nutrients, which are present in the subsurface layer of the equatorial
144 Pacific, forming the main body of the thermocline of this area; station E142-13 is deeply affected by it.
145 The NECC is an important current in the tropical Pacific equatorial current system, transporting warm
146 pool water from the western Pacific to the eastern Pacific; Station E142-19 is mainly affected by it.
147 Furthermore, the area features a substantial upwelling system known as the Mindanao Dome (MD),
148 greatly impacting Station E142-19, situated southeast of the MD.

149 **3.2 Vertical distribution characteristics of POC and $\delta^{13}\text{C}$ -POC**

150 The average POC concentration from the surface to the deep chlorophyll maximum layer (DCM, 0-150
151 m) of the six stations was: E142-19 ($34.12 \pm 3.53 \mu\text{g/L}$) > E142-13 ($31.90 \pm 3.19 \mu\text{g/L}$) > EQ-6 (31.32
152 $\pm 5.27 \mu\text{g/L}$) > E142-3 ($27.77 \pm 4.78 \mu\text{g/L}$) > E142-7 ($27.43 \pm 1.35 \mu\text{g/L}$) > E142-11 ($26.81 \pm 2.25 \mu\text{g/L}$).

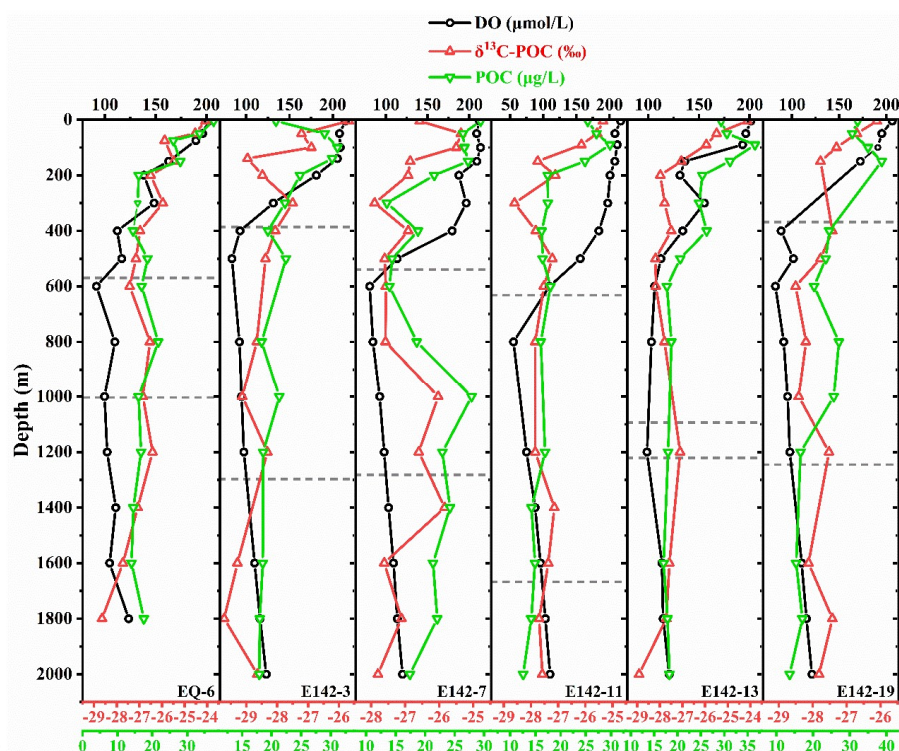
153 The surface POC concentrations at stations E142-13 and EQ-6 were slightly higher than those at other
154 stations. However, the surface POC concentration at station E142-19 was the highest among the six
155 stations because the robust upwelling of MD brought rich nutrients to the surface seawater, alleviating
156 the nitrogen nutrient limitation of the surface water at this station (Gao et al., 2021).

157 The POC concentration of each station demonstrated a decreasing trend with increasing water depth and
158 tended to remain stable in the deep ocean (> 1,000 m) (Fig. 2). The most significant drop in POC
159 concentration occurred between the DCM and 600 m. The seawater within this depth range was abundant
160 in POC and also exhibited relatively high temperature and DO concentration, which enhanced the
161 metabolic activities of heterotrophic organisms, thereby accelerating their utilization of POC (Iversen and
162 Ploug, 2013; Sun et al., 2021). The aerobic degradation of POC led to a significant consumption of DO.

163 Therefore, the change in DO in this water layer was consistent with the change of POC concentration
164 (Fig. 2). It could be inferred that the rapid degradation of POC contributes to the accelerated formation
165 of the oxygen cline. Since the microbial life activities below the oxygen cline were still active, leading
166 to the continued consumption of DO through POC degradation, the DO could not be replenished in time.
167 As a result, the low oxygen zone (where $\text{DO} < 100 \mu\text{mol/L}$) emerged in the middle ocean at all stations
168 (Fig. 2). However, the hypoxic conditions observed at station E142-13 were comparatively less
169 pronounced than those observed at other stations (Fig. 2). This can be attributed to the consistent transport



170 of oxygen and nutrient-rich seawater by the EUC to this station, facilitating oxygen replenishment and
 171 mitigating deoxygenation (Brandt et al., 2021).

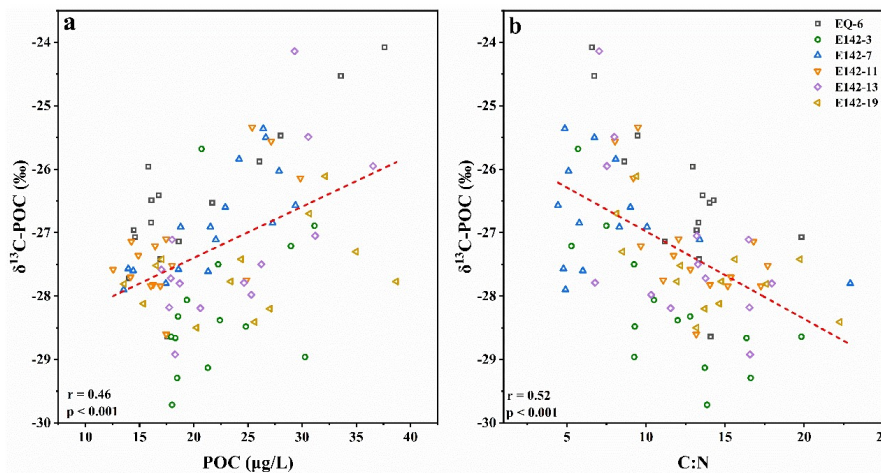


172
 173 **Figure 2.** Vertical distribution of DO, $\delta^{13}\text{C}$ -POC, and POC concentration at each sampling station. The dotted
 174 line marks the hypoxic zone with DO = 100 $\mu\text{mol/L}$ as the boundary.

175 The vertical distribution of $\delta^{13}\text{C}$ -POC closely resembles that of POC concentration (Figs. 2, 3a). This
 176 similarity suggests that specific ^{13}C -enriched components may be preferentially degraded during POC
 177 degradation. Although the molecular composition of oceanic POC cannot be fully identified, it is
 178 generally understood to primarily consist of lipids, amino acids, carbohydrates, nucleic acids, and a small
 179 number of heterogeneous components (Kharbush et al., 2020). The metabolic activity of amino acids and
 180 carbohydrates is higher than lipids, leading microorganisms to preferentially use these compounds as
 181 energy sources, enriching lipids in POC (Hwang et al., 2006; Jeffrey et al., 1983). On the other hand,
 182 compared with lipids, amino acids and carbohydrates exhibit higher $\delta^{13}\text{C}$ values (Hayes, 1993; Hwang
 183 and Druffel, 2003; Schouten et al., 1998). When large quantities of amino acids and carbohydrates
 184 undergo selective degradation, the residual POC will show low $\delta^{13}\text{C}$ characteristics. Therefore, as POC



185 is continuously consumed in the water column, the $\delta^{13}\text{C}$ -POC will gradually decrease. In addition, lipids
 186 have a low nitrogen content in comparison to amino acids and carbohydrates, leading to a relatively high
 187 C:N (Morales et al., 2021). Our findings demonstrated a strong negative correlation between $\delta^{13}\text{C}$ -POC
 188 and C:N (Fig. 3b), which implied that as the water depth increases, $\delta^{13}\text{C}$ -POC decreases while the C:N
 189 in the remaining POC increases. This suggests that selective degradation of POC occurs in our study,
 190 during which amino acids and carbohydrates in the POC were preferentially removed, resulting in a
 191 relative increase in the proportion of lipids in the remaining POC (Druffel et al., 2003).



192
 193 **Figure 3. a. Relationship between $\delta^{13}\text{C}$ -POC and POC concentration; b. Relationship between $\delta^{13}\text{C}$ -POC and**
 194 **C:N**

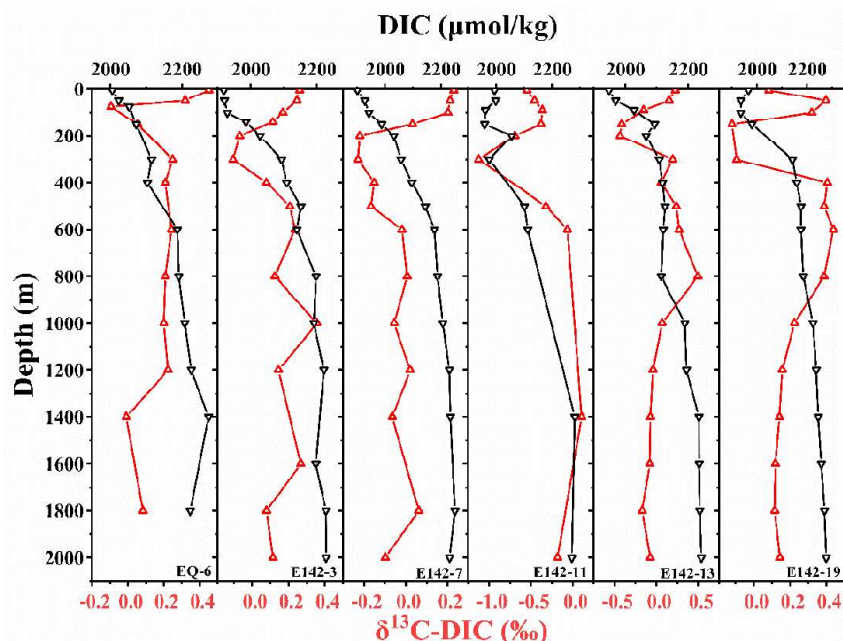
195 3.3 Vertical distribution characteristics of DIC and $\delta^{13}\text{C}$ -DIC

196 The average DIC concentrations of all six stations in the upper ocean, middle ocean, and deep ocean
 197 were 2004 ± 65 , 2147 ± 35 , and 2234 ± 26 $\mu\text{mol/kg}$, respectively. There was a significant increase in
 198 DIC concentration from the upper to the deep ocean (Fig. 4). Affected by photosynthesis, DIC increases
 199 gradually in the upper ocean. In contrast, in the middle ocean, the rapid decomposition of POC released
 200 a large amount of inorganic carbon, causing a rapid increase in DIC throughout the water column. Then,
 201 in deeper layers, only a tiny amount of POC continued to degrade, so the DIC concentration of this layer
 202 increased slowly.

203 Moreover, we observed surface $\delta^{13}\text{C}$ -DIC values ranging from -0.55 to 0.45‰ (average 0.12‰) in the
 204 research region, which is significantly lower than those reported in studies conducted in the Pacific region
 205 in the 1990s (Quay et al., 2017; Quay and Stutsman, 2003). This suggests that the ocean has absorbed



206 more anthropogenic CO₂ as atmospheric CO₂ concentrations have increased over the years. The surface
207 δ¹³C-DIC value of station E142-11 was the lowest among the six stations, only -0.55‰, while the surface
208 δ¹³C-DIC value of station EQ-6 was the highest among the six stations, reaching 0.45‰. This is because
209 station E142-11 was located at the strongest atmospheric CO₂ net sink area, while station EQ-6 was
210 located at the atmospheric CO₂ net source area (Zhong et al., 2022). The sea-air exchange at station E142-
211 11 was sufficient, leading to a lower δ¹³C-DIC value in its surface water, as it was more likely to reach
212 isotopic equilibrium with atmospheric CO₂. In contrast, the surface water of station EQ-6 was more
213 susceptible to seawater mixing and biological primary production influences. The higher δ¹³C-DIC
214 values observed in the surface water of station EQ-6 can be attributed to the isotope fractionation caused
215 by the consumption of a substantial amount of CO₂ by biological primary production (Quay et al., 2003).
216 In analyzing the vertical distribution of δ¹³C-DIC, the findings revealed a rapid decrease in δ¹³C-DIC at
217 each station, mirroring the decline seen in δ¹³C-POC in the upper ocean (0-300 m) (Figs. 4, 5d). Within
218 this depth range, the average decrease in δ¹³C-POC was 2.23‰, while the average decrease of δ¹³C-DIC
219 was 0.30‰, with δ¹³C-DIC reaching its minimum value in the subsurface. However, in the middle ocean
220 layer (300-1,000 m), unlike δ¹³C-POC, δ¹³C-DIC increased first and then stabilized (Fig. 4). Therefore,
221 distinct differences exist in the overall change trends of δ¹³C-DIC and δ¹³C-POC in the ocean water
222 column. Since the mutual conversion between POC and DIC was ongoing, this conversion process will
223 inevitably cause changes in δ¹³C-POC and δ¹³C-DIC. Generally, the variation range of δ¹³C-POC was
224 more significant than that of δ¹³C-DIC, indicating the more complex biogeochemical processes
225 experienced by POC (Meyer et al., 2016; Schmittner et al., 2013).



226

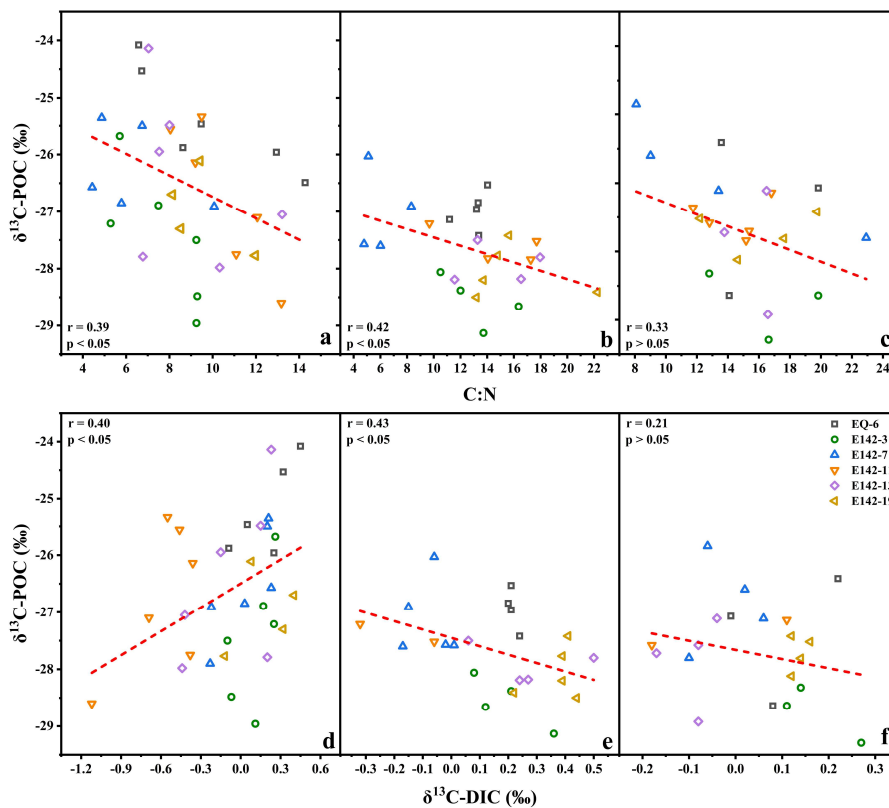
227 **Figure 4.** Vertical distribution of DIC concentration and $\delta^{13}\text{C-DIC}$ at each sampling station. The black line
228 represents DIC, and the red line represents $\delta^{13}\text{C-DIC}$.

229 3.4 Transformation characteristics of POC in different water layers

230 According to the distribution characteristics of $\delta^{13}\text{C-POC}$ and $\delta^{13}\text{C-DIC}$, we divided the ocean water
231 column into three biogeochemical layers: the POC rapid synthesis-degradation layer (RSDL, 0-300 m),
232 the net degradation layer (NDL, 300-1,000 m) and the stable layer (SL, 1,000-2,000 m). Within the RSDL,
233 POC was rapidly degraded while being synthesized. The synthesis rate was greater than the degradation
234 rate from the surface to the DCM layer, while the degradation rate was greater than the synthesis rate
235 below the DCM, reflecting the rapid decrease in photosynthetic rate with depth. In addition, the $\delta^{13}\text{C-}$
236 POC and C:N in this layer exhibited a pronounced negative correlation (Fig. 5a). Therefore, the rapid
237 decrease of $\delta^{13}\text{C-POC}$ in this layer was dominated by the selective degradation of amino acids and
238 carbohydrates. However, at the same time, $\delta^{13}\text{C-POC}$ and $\delta^{13}\text{C-DIC}$ showed a significant positive
239 correlation in this layer (Fig. 5d). Supposing that POC underwent selective degradation, the resulting
240 DIC should exhibit an enrichment in $\delta^{13}\text{C}$. However, contrary to expectations, our findings indicate a
241 decline in $\delta^{13}\text{C-DIC}$ within the RSDL. This perplexing occurrence can be attributed to two primary
242 reasons. On the one hand, the strong sea-air exchange of the surface ocean caused a large amount of



243 heavy ^{13}C generated by degradation to escape from the surface ocean; on the other hand, phytoplankton
244 and photosynthetic bacteria in the upper ocean tended to use the light ^{12}C in the seawater for
245 photosynthesis; thus the $\delta^{13}\text{C}$ -DIC of the surface ocean at all stations was relatively high. However, light
246 intensity diminished with depth increases, causing the photosynthesis rate to slow. Meanwhile, the
247 respiration rate of the biological community was still very fast, resulting in the accumulation of light
248 ^{12}C . Consequently, the $\delta^{13}\text{C}$ -DIC in this layer steadily declined (Ge et al., 2022). In the NDL, the
249 sunlight was pretty weak, and there was almost no photosynthesis. The rate of chemosynthesis of organic
250 carbon was lower than the degradation rate of POC, causing the concentration of POC to continue
251 decreasing. Additionally, the $\delta^{13}\text{C}$ -POC in this layer showed a significant negative correlation with both
252 C:N and $\delta^{13}\text{C}$ -DIC (Fig. 5b, e), suggesting a very active mutual conversion process between POC and
253 DIC. The large amount of selective degradation of amino acids and carbohydrate POC caused the $\delta^{13}\text{C}$ -
254 DIC in this layer to continue to increase. In the SL, the POC concentration remained consistently low.
255 $\delta^{13}\text{C}$ -POC did not correlate significantly with either C:N or $\delta^{13}\text{C}$ -DIC (Fig. 5c, f). This was because the
256 easily degradable components in POC had been completely consumed in the RSDL and NDL, and the
257 remaining components were relatively refractory. As a result, the conversion of POC to DIC was rare in
258 SL, leading to an absence of a clear link between $\delta^{13}\text{C}$ -POC and $\delta^{13}\text{C}$ -DIC.



259
260 **Figure 5. Relationships between $\delta^{13}\text{C-POC}$ and C:N at different depths: (a) 0-300 m, (b) 300-1,000 m, (c)**
261 **1,000-2,000 m, and between $\delta^{13}\text{C-POC}$ and $\delta^{13}\text{C-DIC}$ at different depths: (d) 0-300 m, (e) 300-1,000 m, (f)**
262 **1,000-2,000 m.**

263 4 Conclusions

264 In general, this study investigated the transformation characteristics of POC in the tropical northwest
265 Pacific Ocean based on the $\delta^{13}\text{C}$ perspective. Our findings revealed three distinct stages of POC behavior
266 in the ocean: rapid synthesis-degradation, net degradation, and stable existence. The selective
267 degradation of POC dominated the changes in $\delta^{13}\text{C-POC}$. Following vigorous selective degradation in
268 the RSDL and ND, an increase in the proportion of refractory lipids in POC was observed.
269 Consequently, in the SL, POC was found to be stable with a slow degradation rate. The fractionation of
270 $\delta^{13}\text{C-DIC}$ in the ocean is influenced by both the production and degradation processes of POC. Within
271 the RSDL, $\delta^{13}\text{C-DIC}$ fractionation is predominantly governed by primary production, whereas within the
272 ND, it is primarily influenced by the degradation process of POC.



273 Although we utilized $\delta^{13}\text{C}$ -POC and $\delta^{13}\text{C}$ -DIC to assess the overall transformation characteristics of POC,
274 the specific synthesis and decomposition ratios of POC are still challenging to determine. Further
275 research is needed on the monomer carbon isotopic composition of POC (lipids, amino acids, etc.) to
276 enhance our understanding of the transformation process of POC.

277 **Data Availability.** The data files used in this paper are available at (Tian et al., 2024).

278 **Competing interest.** The authors declare that they have no conflict of interest.

279 **Author contribution.** Detong Tian: Investigation, Data Curation, Writing-original draft. Xuegang Li
280 and Jinming Song: Conceptualization, Funding acquisition, Writing-review & editing. Jun Ma, Funding
281 acquisition. Huamao Yuan, Liqin Duan.; Writing - Review & Editing.

282 **Acknowledgments.** This work was supported by the National Key Research and Development Program
283 (grant no. 2022YFC3104305), National Natural Science Foundation of China (grant nos.42176200,
284 42206135); Laoshan Laboratory (grant nos. LSKJ202204001, LSKJ202205001). We appreciate the
285 crews of the R/V *Kexue* for sampling assistance during the cruise of NORC2021-09 supported by the
286 National Natural Science Foundation of China (project no. 42049909).



287 **References**

- 288 Brandt, P., Hahn, J., Schmidtko, S., Tuchen, F. P., Kopte, R., Kiko, R., Bourlès, B., Czeschel, R., and Dengler,
289 M.: Atlantic Equatorial Undercurrent intensification counteracts warming-induced deoxygenation,
290 Nature Geoscience, 14, 278-282, <http://doi.org/10.1038/s41561-021-00716-1>, 2021.
- 291 Bryan, J. R., Riley, J. P., and Williams, P. J. L.: A winkler procedure for making precise measurements of
292 oxygen concentration for productivity and related studies, J. Exp. Mar. Biol. Ecol., 21, 191-197,
293 [http://doi.org/10.1016/0022-0981\(76\)90114-3](http://doi.org/10.1016/0022-0981(76)90114-3), 1976.
- 294 Close, H. G. and Henderson, L. C.: Open-Ocean Minima in $\delta^{13}\text{C}$ Values of Particulate Organic Carbon in
295 the Lower Euphotic Zone, Frontiers in Marine Science, 7, <http://doi.org/10.3389/fmars.2020.540165>,
296 2020.
- 297 Ding, L., Qi, Y., Shan, S., Ge, T., Luo, C., and Wang, X.: Radiocarbon in Dissolved Organic and Inorganic
298 Carbon of the South China Sea, Journal of Geophysical Research: Oceans, 125,
299 <http://doi.org/10.1029/2020jc016073>, 2020.
- 300 Druffel, E. R. M., Bauer, J. E., Griffin, S., and Hwang, J.: Penetration of anthropogenic carbon into organic
301 particles of the deep ocean, Geophysical Research Letters, 30, <http://doi.org/10.1029/2003gl017423>,
302 2003.
- 303 Eadie, B. J. and Jeffrey, L. M.: $\delta^{13}\text{C}$ analyses of oceanic particulate organic matter, Marine Chemistry, 1,
304 199-209, [http://doi.org/10.1016/0304-4203\(73\)90004-2](http://doi.org/10.1016/0304-4203(73)90004-2), 1973.
- 305 Friedlingstein, P., O'Sullivan, M., Jones, M. W., Andrew, R. M., Bakker, D. C. E., Hauck, J., Landschützer,
306 P., Le Quéré, C., Lujikx, I. T., Peters, G. P., Peters, W., Pongratz, J., Schwingshackl, C., Sitch, S., Canadell, J.
307 G., Ciais, P., Jackson, R. B., Alin, S. R., Anthoni, P., Barbero, L., Bates, N. R., Becker, M., Bellouin, N.,
308 Decharme, B., Bopp, L., Brasika, I. B. M., Cadule, P., Chamberlain, M. A., Chandra, N., Chau, T.-T.-T.,
309 Chevallier, F., Chini, L. P., Cronin, M., Dou, X., Enyo, K., Evans, W., Falk, S., Feely, R. A., Feng, L., Ford, D.
310 J., Gasser, T., Ghattas, J., Gkritzalis, T., Grassi, G., Gregor, L., Gruber, N., Gürses, Ö., Harris, I., Hefner, M.,
311 Heinke, J., Houghton, R. A., Hurtt, G. C., Iida, Y., Ilyina, T., Jacobson, A. R., Jain, A., Jarníková, T., Jersild,
312 A., Jiang, F., Jin, Z., Joos, F., Kato, E., Keeling, R. F., Kennedy, D., Klein Goldewijk, K., Knauer, J., Korsbakken,
313 J. I., Körtzinger, A., Lan, X., Lefèvre, N., Li, H., Liu, J., Liu, Z., Ma, L., Marland, G., Mayot, N., McGuire, P.
314 C., McKinley, G. A., Meyer, G., Morgan, E. J., Munro, D. R., Nakaoka, S.-I., Niwa, Y., O'Brien, K. M., Olsen,
315 A., Omar, A. M., Ono, T., Paulsen, M., Pierrot, D., Pockock, K., Poulter, B., Powis, C. M., Rehder, G.,



316 Resplandy, L., Robertson, E., Rödenbeck, C., Rosan, T. M., Schwinger, J., Séférian, R., Smallman, T. L.,
317 Smith, S. M., Sospedra-Alfonso, R., Sun, Q., Sutton, A. J., Sweeney, C., Takao, S., Tans, P. P., Tian, H.,
318 Tilbrook, B., Tsujino, H., Tubiello, F., van der Werf, G. R., van Ooijen, E., Wanninkhof, R., Watanabe, M.,
319 Wilmart-Rousseau, C., Yang, D., Yang, X., Yuan, W., Yue, X., Zaehle, S., Zeng, J., and Zheng, B.: Global
320 Carbon Budget 2023, *Earth System Science Data*, 15, 5301-5369, [http://doi.org/10.5194/essd-15-5301-](http://doi.org/10.5194/essd-15-5301-2023)
321 [2023](http://doi.org/10.5194/essd-15-5301-2023), 2023.

322 Gao, W., Wang, Z., Li, X., and Huang, H.: The increased storage of suspended particulate matter in the
323 upper water of the tropical Western Pacific during the 2015/2016 super El Niño event, *Journal of*
324 *Oceanology and Limnology*, 39, 1675-1689, <http://doi.org/10.1007/s00343-021-0362-0>, 2021.

325 Ge, T., Luo, C., Ren, P., Zhang, H., Fan, D., Chen, H., Chen, Z., Zhang, J., and Wang, X.: Stable carbon
326 isotopes of dissolved inorganic carbon in the Western North Pacific Ocean: Proxy for water mixing and
327 dynamics, *Frontiers in Marine Science*, 9, <http://doi.org/10.3389/fmars.2022.998437>, 2022.

328 Guo, J., Zhou, B., Achterberg, E. P., Yuan, H., Song, J., Duan, L., and Li, X.: Rapid Cycling of Bacterial
329 Particulate Organic Matter in the Upper Layer of the Western Pacific Warm Pool, *Geophysical Research*
330 *Letters*, 50, <http://doi.org/10.1029/2023gl102896>, 2023.

331 Hayes, J. M.: Factors controlling ¹³C contents of sedimentary organic compounds: Principles and
332 evidence, *Marine Geology*, 113, 111-125, [http://doi.org/10.1016/0025-3227\(93\)90153-m](http://doi.org/10.1016/0025-3227(93)90153-m), 1993.

333 Herndl, G. J., Bayer, B., Baltar, F., and Reinthaler, T.: Prokaryotic Life in the Deep Ocean's Water Column,
334 *Ann Rev Mar Sci*, 15, 461-483, <http://doi.org/10.1146/annurev-marine-032122-115655>, 2023.

335 Hernes, P. J. and Benner, R.: Transport and diagenesis of dissolved and particulate terrigenous organic
336 matter in the North Pacific Ocean, *Deep Sea Research Part I: Oceanographic Research Papers*, 49, 2119-
337 2132, [http://doi.org/10.1016/s0967-0637\(02\)00128-0](http://doi.org/10.1016/s0967-0637(02)00128-0), 2002.

338 Hu, D., Wu, L., Cai, W., Gupta, A. S., Ganachaud, A., Qiu, B., Gordon, A. L., Lin, X., Chen, Z., Hu, S., Wang,
339 G., Wang, Q., Sprintall, J., Qu, T., Kashino, Y., Wang, F., and Kessler, W. S.: Pacific western boundary
340 currents and their roles in climate, *Nature*, 522, 299-308, <http://doi.org/10.1038/nature14504>, 2015.

341 Hwang, J. and Druffel, E. R.: Lipid-like material as the source of the uncharacterized organic carbon in
342 the ocean?, *Science*, 299, 881-884, <http://doi.org/10.1126/science.1078508>, 2003.

343 Hwang, J., Druffel, E. R. M., Eglinton, T. I., and Repeta, D. J.: Source(s) and cycling of the nonhydrolyzable
344 organic fraction of oceanic particles, *Geochimica et Cosmochimica Acta*, 70, 5162-5168,
345 <http://doi.org/10.1016/j.gca.2006.07.020>, 2006.



- 346 Iversen, M. H. and Ploug, H.: Temperature effects on carbon-specific respiration rate and sinking velocity
347 of diatom aggregates – potential implications for deep ocean export processes, *Biogeosciences*, 10,
348 4073-4085, <http://doi.org/10.5194/bg-10-4073-2013>, 2013.
- 349 Jeffrey, A. W. A., Pflaum, R. C., Brooks, J. M., and Sackett, W. M.: Vertical trends in particulate organic
350 carbon ^{13}C : ^{12}C ratios in the upper water column, *Deep Sea Research Part A. Oceanographic Research*
351 *Papers*, 30, 971-983, [http://doi.org/10.1016/0198-0149\(83\)90052-3](http://doi.org/10.1016/0198-0149(83)90052-3), 1983.
- 352 Jia, Q., Li, T., Xiong, Z., Steinke, S., Jiang, F., Chang, F., and Qin, B.: Hydrological variability in the western
353 tropical Pacific over the past 700 kyr and its linkage to Northern Hemisphere climatic change,
354 *Palaeogeography, Palaeoclimatology, Palaeoecology*, 493, 44-54,
355 <http://doi.org/10.1016/j.palaeo.2017.12.039>, 2018.
- 356 Jian, Z., Wang, Y., Dang, H., Mohtadi, M., Rosenthal, Y., Lea, D. W., Liu, Z., Jin, H., Ye, L., Kuhnt, W., and
357 Wang, X.: Warm pool ocean heat content regulates ocean-continent moisture transport, *Nature*, 612,
358 92-99, <http://doi.org/10.1038/s41586-022-05302-y>, 2022.
- 359 Kharbush, J. J., Close, H. G., Van Mooy, B. A. S., Arnosti, C., Smittenberg, R. H., Le Moigne, F. A. C.,
360 Mollenhauer, G., Scholz-Böttcher, B., Obrecht, I., Koch, B. P., Becker, K. W., Iversen, M. H., and Mohr, W.:
361 Particulate Organic Carbon Deconstructed: Molecular and Chemical Composition of Particulate Organic
362 Carbon in the Ocean, *Frontiers in Marine Science*, 7, <http://doi.org/10.3389/fmars.2020.00518>, 2020.
- 363 Lee, C., Wakeham, S. G., and I. Hedges, J.: Composition and flux of particulate amino acids and
364 chloropigments in equatorial Pacific seawater and sediments, *Deep Sea Research Part I: Oceanographic*
365 *Research Papers*, 47, 1535-1568, [http://doi.org/10.1016/s0967-0637\(99\)00116-8](http://doi.org/10.1016/s0967-0637(99)00116-8), 2000.
- 366 Longhurst, A. R. and Glen Harrison, W.: The biological pump: Profiles of plankton production and
367 consumption in the upper ocean, *Progress in Oceanography*, 22, 47-123, [http://doi.org/10.1016/0079-6611\(89\)90010-4](http://doi.org/10.1016/0079-6611(89)90010-4), 1989.
- 369 Ma, J., Song, J., Li, X., Yuan, H., Li, N., Duan, L., and Wang, Q.: Control factors of DIC in the Y3 seamount
370 waters of the Western Pacific Ocean, *Journal of Oceanology and Limnology*, 38, 1215-1224,
371 <http://doi.org/10.1007/s00343-020-9314-3>, 2020.
- 372 Ma, J., Song, J., Li, X., Wang, Q., Zhong, G., Yuan, H., Li, N., and Duan, L.: The OMZ and Its Influence on
373 POC in the Tropical Western Pacific Ocean: Based on the Survey in March 2018, *Frontiers in Earth*
374 *Science*, 9, <http://doi.org/10.3389/feart.2021.632229>, 2021.
- 375 Meyer, K. M., Ridgwell, A., and Payne, J. L.: The influence of the biological pump on ocean chemistry:



376 implications for long-term trends in marine redox chemistry, the global carbon cycle, and marine animal
377 ecosystems, *Geobiology*, 14, 207-219, <http://doi.org/10.1111/gbi.12176>, 2016.

378 Morales, M., Afalo, C., and Bernard, O.: Microalgal lipids: A review of lipids potential and quantification
379 for 95 phytoplankton species, *Biomass and Bioenergy*, 150,
380 <http://doi.org/10.1016/j.biombioe.2021.106108>, 2021.

381 Passos, J. G., Soares, L. F., Sumida, P. Y. G., Bendia, A. G., Nakamura, F. M., Pellizari, V. H., and Signori, C.
382 N.: Contribution of chemoautotrophy and heterotrophy to the microbial carbon cycle in the
383 Southwestern Atlantic Ocean, *Ocean and Coastal Research*, 70, [http://doi.org/10.1590/2675-
384 2824070.22137jgp](http://doi.org/10.1590/2675-2824070.22137jgp), 2022.

385 Quay, P. and Stutsman, J.: Surface layer carbon budget for the subtropical N. Pacific: constraints at
386 station ALOHA, *Deep Sea Research Part I: Oceanographic Research Papers*, 50, 1045-1061,
387 [http://doi.org/10.1016/s0967-0637\(03\)00116-x](http://doi.org/10.1016/s0967-0637(03)00116-x), 2003.

388 Quay, P., Sonnerup, R., Munro, D., and Sweeney, C.: Anthropogenic CO₂ accumulation and uptake rates
389 in the Pacific Ocean based on changes in the ¹³C/¹²C of dissolved inorganic carbon, *Global
390 Biogeochemical Cycles*, 31, 59-80, <http://doi.org/10.1002/2016gb005460>, 2017.

391 Quay, P., Sonnerup, R., Westby, T., Stutsman, J., and McNichol, A.: Changes in the ¹³C/¹²C of dissolved
392 inorganic carbon in the ocean as a tracer of anthropogenic CO₂ uptake, *Global Biogeochemical Cycles*,
393 17, <http://doi.org/10.1029/2001gb001817>, 2003.

394 Radenac, M.-H., Messié, M., Léger, F., and Bosc, C.: A very oligotrophic zone observed from space in the
395 equatorial Pacific warm pool, *Remote Sensing of Environment*, 134, 224-233,
396 <http://doi.org/10.1016/j.rse.2013.03.007>, 2013.

397 Reinthaler, T., van Aken, H. M., and Herndl, G. J.: Major contribution of autotrophy to microbial carbon
398 cycling in the deep North Atlantic's interior, *Deep Sea Research Part II: Topical Studies in Oceanography*,
399 57, 1572-1580, <http://doi.org/10.1016/j.dsr2.2010.02.023>, 2010.

400 Sannigrahi, P., Ingall, E. D., and Benner, R.: Cycling of dissolved and particulate organic matter at station
401 Aloha: Insights from ¹³C NMR spectroscopy coupled with elemental, isotopic and molecular analyses,
402 *Deep Sea Research Part I: Oceanographic Research Papers*, 52, 1429-1444,
403 <http://doi.org/10.1016/j.dsr.2005.04.001>, 2005.

404 Schmittner, A., Gruber, N., Mix, A. C., Key, R. M., Tagliabue, A., and Westberry, T. K.: Biology and air-sea
405 gas exchange controls on the distribution of carbon isotope ratios ($\delta^{13}\text{C}$) in the



- 406 ocean, Biogeosciences, 10, 5793-5816, <http://doi.org/10.5194/bg-10-5793-2013>, 2013.
- 407 Schönau, M. C., Rudnick, D. L., Gopalakrishnan, G., Cornuelle, B. D., and Qiu, B.: Mean, Annual, and
408 Interannual Circulation and Volume Transport in the Western Tropical North Pacific From the Western
409 Pacific Ocean State Estimates (WPOSE), Journal of Geophysical Research: Oceans, 127,
410 <http://doi.org/10.1029/2021jc018213>, 2022.
- 411 Schouten, S., Klein Breteler, W. C. M., Blokker, P., Schogt, N., Rijpstra, W. I. C., Grice, K., Baas, M., and
412 Sinninghe Damsté, J. S.: Biosynthetic effects on the stable carbon isotopic compositions of algal lipids:
413 implications for deciphering the carbon isotopic biomarker record, Geochimica et Cosmochimica Acta,
414 62, 1397-1406, [http://doi.org/10.1016/s0016-7037\(98\)00076-3](http://doi.org/10.1016/s0016-7037(98)00076-3), 1998.
- 415 Smith, C. R., De Leo, F. C., Bernardino, A. F., Sweetman, A. K., and Arbizu, P. M.: Abyssal food limitation,
416 ecosystem structure and climate change, Trends Ecol Evol, 23, 518-528,
417 <http://doi.org/10.1016/j.tree.2008.05.002>, 2008.
- 418 Song, J.: Biogeochemical Processes of Biogenic Elements in China Marginal Seas, Advanced Topics in
419 Science and Technology in China, Springer Berlin, Heidelberg, 662 pp.,
420 <http://doi.org/https://doi.org/10.1007/978-3-642-04060-3>, 2010.
- 421 Sun, Q., Song, J., Li, X., Yuan, H., and Wang, Q.: The bacterial diversity and community composition
422 altered in the oxygen minimum zone of the Tropical Western Pacific Ocean, Journal of Oceanology and
423 Limnology, 39, 1690-1704, <http://doi.org/10.1007/s00343-021-0370-0>, 2021.
- 424 Takahashi, T., Sutherland, S. C., Wanninkhof, R., Sweeney, C., Feely, R. A., Chipman, D. W., Hales, B.,
425 Friederich, G., Chavez, F., Sabine, C., Watson, A., Bakker, D. C. E., Schuster, U., Metzl, N., Yoshikawa-
426 Inoue, H., Ishii, M., Midorikawa, T., Nojiri, Y., Körtzinger, A., Steinhoff, T., Hoppema, M., Olafsson, J.,
427 Arnarson, T. S., Tilbrook, B., Johannessen, T., Olsen, A., Bellerby, R., Wong, C. S., Delille, B., Bates, N. R.,
428 and de Baar, H. J. W.: Climatological mean and decadal change in surface ocean pCO₂, and net sea-air
429 CO₂ flux over the global oceans, Deep Sea Research Part II: Topical Studies in Oceanography, 56, 554-
430 577, <http://doi.org/10.1016/j.dsr2.2008.12.009>, 2009.
- 431 Tian, D., Li, X., Song, J., Ma, J, Yuan, H & Duan, L.: Vertical layering and transformation of particulate
432 organic carbon in the tropical Northwestern Pacific Ocean waters based on $\delta^{13}C$, Figshare [Dataset].
433 <https://doi.org/10.6084/m9.figshare.26197808>, 2024
- 434 Turner, J. T.: Zooplankton fecal pellets, marine snow, phytodetritus and the ocean's biological pump,
435 Progress in Oceanography, 130, 205-248, <http://doi.org/10.1016/j.poccean.2014.08.005>, 2015.



- 436 Walsh, D. A., Zaikova, E., Howes, C. G., Song, Y. C., Wright, J. J., Tringe, S. G., Tortell, P. D., and Hallam, S.
437 J.: Metagenome of a versatile chemolithoautotroph from expanding oceanic dead zones, *Science*, 326,
438 578-582, <http://doi.org/10.1126/science.1175309>, 2009.
- 439 Wu, L., Liu, Z., Liu, Y., Liu, Q., and Liu, X.: Potential global climatic impacts of the North Pacific Ocean,
440 *Geophysical Research Letters*, 32, <http://doi.org/10.1029/2005gl024812>, 2005.
- 441 Zhong, G., Li, X., Song, J., Qu, B., Wang, F., Wang, Y., Zhang, B., Tian, D., Ma, J., Yuan, H., Duan, L., Li, N.,
442 Wang, Q., and Xing, J.: The increasing big gap of carbon sink between the western and eastern Pacific
443 in the last three decades, *Frontiers in Marine Science*, 9, <http://doi.org/10.3389/fmars.2022.1088181>,
444 2022.
- 445 Zuo, J., Song, J., Yuan, H., Li, X., Li, N., and Duan, L.: Impact of Kuroshio on the dissolved oxygen in the
446 East China Sea region, *Journal of Oceanology and Limnology*, 37, 513-524,
447 <http://doi.org/10.1007/s00343-019-7389-5>, 2018.